4142–4157 *Nucleic Acids Research, 2017, Vol. 45, No. 7* *Published online 20 December 2016*
doi: 10.1093/nar/gkw1287

MicroRNA-202 maintains spermatogonial stem cells by inhibiting cell cycle regulators and RNA binding proteins

Jian Chen[1,2,†], Tanxi Cai[2,3,†], Chunwei Zheng[1,2], Xiwen Lin[1], Guojun Wang[1], Shangying Liao[1], Xiuxia Wang[1], Haiyun Gan[1], Daoqin Zhang[1,2], Xiangjing Hu[1,2], Si Wang[1], Zhen Li[1], Yanmin Feng[1,2], Fuquan Yang[2,3,*] and Chunsheng Han[1,2,*]

[1]State Key Laboratory of Stem Cell and Reproductive Biology, Institute of Zoology, Chinese Academy of Sciences, Beijing 100101, China, [2]University of Chinese Academy of Sciences, Beijing 100049, China and [3]The Key Laboratory of Protein and Peptide Pharmaceuticals & Laboratory of Proteomics, Institute of Biophysics, Chinese Academy of Sciences, Beijing 100101, China

Received October 20, 2016; Revised December 06, 2016; Editorial Decision December 07, 2016; Accepted December 13, 2016

ABSTRACT

miRNAs play important roles during mammalian spermatogenesis. However, the function of most miRNAs in spermatogenesis and the underlying mechanisms remain unknown. Here, we report that miR-202 is highly expressed in mouse spermatogonial stem cells (SSCs), and is oppositely regulated by Glial cell-Derived Neurotrophic Factor (GDNF) and retinoic acid (RA), two key factors for SSC self-renewal and differentiation. We used inducible CRISPR-Cas9 to knockout miR-202 in cultured SSCs, and found that the knockout SSCs initiated premature differentiation accompanied by reduced stem cell activity and increased mitosis and apoptosis. Target genes were identified with iTRAQ-based proteomic analysis and RNA sequencing, and are enriched with cell cycle regulators and RNA-binding proteins. *Rbfox2* and *Cpeb1* were found to be direct targets of miR-202 and *Rbfox2* but not *Cpeb1*, is essential for the differentiation of SSCs into meiotic cells. Accordingly, an SSC fate-regulatory network composed of signaling molecules of GDNF and RA, miR-202 and diverse downstream effectors has been identified.

INTRODUCTION

Spermatogenesis is a unique developmental process whereby highly specialized haploid sperm are generated from their diploid spermatogonial precursors via the meiosis of spermatocytes (1). It has been recognized as an ideal model for investigating many fundamental biological processes such as self-renewal and differentiation of stem cells, transcriptional and post-transcriptional regulation of gene expression, and the replication, recombination and epigenetic modification of DNAs. During spermatogenesis, multiple types of intermediate cells are generated from spermatogonial stem cells (SSCs). For example, mouse spermatogonia include undifferentiated, differentiating and differentiated spermatogonia, all of which undergo mitotic divisions to amplify cell population as well as step-wise differentiation to prepare for meiosis (2,3). SSCs are a small subset of the heterogeneous undifferentiated spermatogonia. Several growth factors such as Glial cell-Derived Neurotrophic Factor (GDNF), bFGF, IGF are essential for the self-renewal of SSCs while other substance such as retinoic acid (RA) is critical for spermatogonial differentiation and meiosis initiation (4). The GDNF receptor subunit GFRα1 and some intracellular proteins such as OCT4, LIN28A, PLZF, NANOS3 are marker proteins of the undifferentiated spermatogonia while c-KIT is a hallmark of differentiating spermatogonia. The expression of STRA8, DAZL, SYCP3, PRDM9 AND DMC1 indicates the initiation and undergoing of meiosis (5). Spermatogenesis is driven by the stage-specific expression of genes that are regulated transcriptionally and

*To whom correspondence should be addressed. Tel: +86 10 64807105; Fax: +86 10 64807105; Email: hancs@ioz.ac.cn
Correspondence may also be addressed to Fuquan Yang. Tel: +86 10 64888581; Fax: +86 10 64871293; Email: fqyang@sun5.ibp.ac.cn
†These authors contributed equally to this paper as the first authors.
Present addresses:
Haiyun Gan, Irving Cancer Research Center, Columbia University Medical Center, NY 10032, USA.
Si Wang, National Laboratory of Biomacromolecules, Institute of Biophysics, Chinese Academy of Sciences, Beijing 100101, China.

post-transcriptionally (6), and it involves the expression of a large number of highly or specifically expressed coding and non-coding genes in various spermatogenic cells.

miRNAs are believed to be essential for spermatogenesis as conditional knockout (KO) of dicer in either primordial germ cells or undifferentiated spermatogonia resulted in infertility (7–11). Accumulated defects in spermatogenic cells such as reduced proliferation, increased apoptosis, elevated retrotransposon activity, delayed meiosis progression and abnormal post-meiotic development are observed, probably due to the loss of diverse miRNAs. As the production of both miRNAs and endo-siRNAs is depend on DICER while only the production of miRNAs is dependent on DROSHA and DGCR8, the essential role of miRNAs in spermatogenesis has also been confirmed by the similar infertile phenotypes of conditional KO mice of either *Drosha* or *Dgcr8* (12,13).

The expression and function of some individual miRNAs or miRNA clusters during spermatogenesis have been reported (14,15). The function of most studied miRNAs were either inferred from the regulatory relationships between miRNAs and key regulators of spermatogenesis or based on the *in vitro* results of inhibition or overexpression assays (16–23). Few miRNAs were examined for their *in vivo* function by evaluating the phenotypes of their gene KO mice. For example, conditional KO of the miRNA cluster Mirc1, which is highly expressed in undifferentiated spermatogonia, resulted in impaired spermatogenesis indicated by the appearance of Sertoli cell-only tubules (24). KO mice of miR-449 have no phenotypic abnormality, which was probably due to the compensational effect of miR-34b/c (25).

Despite their important roles in mammalian spermatogenesis, comprehensive transcriptomic profiles of miRNAs in various spermatogenic cells are not available. The expression of hundreds of miRNAs in mouse testes was first reported by using a large scale molecular cloning method (26). Microarray analyses of miRNA expression in testes or spermatogenic cells were also reported, but only a small number of differentially expressed miRNAs have been identified (14,27–30). An RNA sequencing study reported the expression of about 700 miRNAs and their isoforms due to RNA editing in mouse testis at different developmental stages (31). A similar study identified about 500 miRNAs in each of the isolated $THY1^+$ SSC-enriched germ cells, $THY1^-$ somatic cells and cultured SSCs derived from $THY1^+$ cells (32). However, these studies failed to profile miRNAs explicitly in various isolated spermatogenic cells such as spermatogonia, spermatocytes and spermatids.

We previously used RNA sequencing to study the expression of small RNAs including piRNAs and miRNAs and found that miRNAs are much more abundant in spermatogonia than in other cell types (33). In the present study, we re-analyzed that dataset deposited in the GEO database as well as a multi-organ dataset generated by Kuchen *et al.* (34), and compiled a complete list of miRNAs that are expressed in spermatogenic cells and reported their organ and cell type specificities. We showed that miR-202-3p and -5p, two miRNAs highly expressed in the testis and spermatogenic cells, were differentially regulated by GDNF and RA, which are key factors for the self-renewal and differentiation of SSCs. miR-202 prevented SSCs from premature differentiation by suppressing the expression of multiple target genes such as cell cycle regulators and RNA binding proteins. We identified *Rbfox2* and *Cpeb1* as two direct target genes of miR-202 and found that the knockdown of *Rbfox2* but not *Cpeb1* blocked meiosis initiation of cultured SSCs. These results have revealed a miR-202-centered regulatory network that controls the fate of SSCs, and they also contribute to the understanding the roles of miRNAs in stem cell fate determination.

MATERIALS AND METHODS

Animal breeding and cell cultures

All animals used in this study were bred by following the guidelines of the Animal Care and Use Committee of the Institute of Zoology, Chinese Academy of Sciences. F1 pups derived from DBA/2 and C57BL6 mice were used for isolation of SSCs and transplantation assays.

Establishment, maintenance and differentiation induction of lines of mouse SSCs

Establishment and maintenance of SSCs followed the protocols developed by Kanatsu–Shinohara *et al.* and Kubota *et al.* (35,36) with modifications from our laboratory (37). Briefly, seminiferous tubules of testis from pup mice of 5–7 days post-partum (dpp) were digested with 1 mg/ml collagenase IV and 1 mg/ml DNase I at 37°C for 5 min, and then centrifuged at 20 *g* for 1 min. The supernatant containing Leydig cells was removed, and the precipitation of tubules was suspended in mouse embryo fibroblasts (MEF) medium with several pipetting and plated onto dishes. One day later, somatic cells grew out of the tubules, on which SSCs were loosely attached. Then, the SSCs were collected by gentle pipetting and centrifugation. The collected cells were cultured in SSC medium, which contains 20 ng/ml GDNF, 5 ng/ml bFGF and 5 μg/ml insulin, on mitomycin-inactivated MEF. The contaminated somatic cells were removed after three passages and the SSCs were subsequently maintained in SSC medium for at least several months.

To test the effects of growth factors and RA on the levels of miR-202-3p and miR-202-5p, SSCs were treated with GDNF, bFGF or insulin for 12 h after overnight (∼18 h) withdrawal from growth factors (-Factors) or treated with RA for 24 h, followed by real-time PCR.

miRNA inhibitors or siRNAs were transfected into SSCs at the concentration of 100 nM by RNAiMAX (Invitrogen, Thermo Fisher Scientific), following the standard manufacture protocol.

Differentiation induction of SSCs follows our recently reported procedure (4). Briefly, SSCs were plated on Sertoli cells and one day later, treated with 100 nM RA. The immunostaining of SYCP3 was used to assess the ability for entry of meiosis.

Transplantation of SSCs

Transplantation of SSCs into recipient testes was conducted by following procedures previously described (37). One month after transplantation, mice transplanted with iKO-SSCs or Ctr-iKO-SSCs were treated with Dox water containing 2 mg/ml Doxycycline (Dox, Clontech, Takara) in

5% sucrose that was refreshed every 3 days for three times (38). Six weeks after treatment, the testes were sampled for analysis.

Clonal expansion of SSCs from single cells

SSCs were seeded into a 3.5 cm dish on MEF feeder at a density of 100 cells/cm^2. Ten days later, colonies expanded from single cells were picked and plated into the wells of 96-well plate for further amplification.

Plasmid construction and lentivirus production

We obtained the Tet-On Cas9-expressing lentivirus vector pCW-Cas9 (39) from Addgene (50661). Lentiviral production was performed as described previously (40), using the packaging plasmid pMD2.G and the envelope plasmid psPAX2.

We developed iCas9-SSC by infecting SSCs with Cas9 lentivirus and screening puromycin-resistant SSCs using 1 μg/ml puromycin for 14 days. The expression of Flag-Cas9 after adding Dox (10 μg/ml, Clontech, Takara) was identified by Western blot using a Flag antibody.

To develop the iKO-SSCs and Ctr-iKO-SSCs, we first cloned the two gRNAs targeting miRNA into PGL3-U6 (Addgene, 51133), and then amplified the two U6-gRNA cassettes by PCRs and inserted them into modified pLL3.7 vector (Addgene, 11795), together with the EF1a-EGFP cassette. iCas9-SSCs were transfected by the iKO and Ctr-iKO lentivirus and the EGFP-positive cells were sorted by flow cytometer.

For the ectopic expression of miR-202, we placed the U6-miR-202 cassette into the iKO plasmid to derive the iKO-OE plasmid. We also placed the U6-miR-202 into a lentiviral plasmid harboring EF1-Tomato cassette to derive the iKO-SC-OE construct.

iTRAQ labeling and LC-MS/MS analysis

Cells were washed with phosphate-buffered saline (PBS) twice and harvested by scraping in ice-cold RIPA supplemented with protease inhibitor cocktail (Roche). Cell lysates were centrifuged at 16 000 g for 15 min at 4°C to remove cell debris. Supernatants were collected and stored at −80°C until use. Cell lysates were denatured according to the FASP procedure with minor modifications (41). Briefly, the cell lysates were transferred to Amicon-0.5 ultrafiltration units, and the buffer was exchanged with UA buffer (8 M urea, 0.1 M Tris, pH 8.5) three times. Protein samples were reduced with 10 mM dithiothreitol at 37°C for 1 h and then alkylated with 50 mM iodoacetamide at room temperature for 1 h (in the dark). The buffer of the denatured protein samples was then exchanged with UA buffer three times and exchanged with 50 mM tetraethylammonium bromide (TEAB) twice. Proteins were recovered by reverse centrifugation at 1000 *g* for 2 min and resolved in 50 mM TEAB. Protein concentrations were determined in triplicate using the bicinchoninic acid method (Thermo Scientific Pierce) according to the manufacturer's instructions.

One hundred micrograms of lysate proteins from iKO-SC-1, iKO-SC-2 and two samples of iKO-OE-SSCs were digested with trypsin at 37°C overnight. Then, the tryptic peptide was labeled with iTRAQ reagent as showed in Figure 6A according to the manufacturer's instructions. Following labeling, the eight tagged peptide samples were pooled together and stored at −80°C until MS analysis.

After desalted by C_{18} SPE cartridges (Waters), the labeled peptides were fractionated using YMC-Triart C_{18} basic reversed-phase liquid chromatography column (250 × 4.6 mm, 5 μm particles, YMC). Eluates were collected every 75 s, and a total number of 57 fractions were obtained. The first five fractions were discarded because most of the excess labeling reagent was eluted during these fractions. The remaining 52 fractions were combined into 13 fractions by merging fraction 1, 14, 27 and 40; fraction 2, 15, 28 and 41; and so on. Then, all fractions were dried in a vacuum concentrator and stored at −20°C until further analysis.

All mass spectrometry data were collected on a Q-Exactive mass spectrometer (Thermo Fisher Scientific) coupled with an Easy-nLC system (Thermo Fisher Scientific). Each fraction of tryptic peptides was resuspended in 0.1% formic acid and separated on EASY-Spray column (C_{18}, 2 μm particle size, 100 Å pore size, 75 μm id × 50 cm length, Thermo Fisher Scientific). Samples were resolved with a linear gradient of solvent B (100% ACN, 0.1% formic acid); 5–50% over 76 min, 50–90% over 12 min at a flow rate of 300 nl/min. The separated peptide ions eluted from the analytic column entered into the mass spectrometer at an electrospray voltage of 2.1 kV. All MS/MS spectra were acquired in a data-dependent mode for fragmentation of the 10 most abundant peaks from the full MS scan with 30% normalized collision energy. The dynamic exclusion duration was set at 20 s and the isolation mass width was 2.5 Da. MS spectra were acquired with a mass range of 400–1800 m/z and a resolution of 70 000 at m/z 200. MS/MS resolution was acquired at a resolution of 17 500.

Protein identification and quantification

The LC-MS/MS data were analyzed using Proteome Discoverer (Version 1.4, Thermo Fisher Scientific) against the Uniprot KB mouse database (released on September, 2013) with 50,287 entries, into which 175 commonly observed contaminants and all the reverse sequences were added. Search parameters included: precursor ions mass tolerance of 10 ppm (monoisotopic mass), fragment ions mass tolerance of 0.02 Da (monoisotopic mass), a fixed modifications of cysteine carbamidomethylation and iTRAQ 8-plex labeling at the N-terminus and lysine residues, and a variable modification of addition of 15.999 Da on methionine (oxidation). The search results were passed through additional filters before exporting the data. For protein identification, the filters were set as follows: peptides with more than two unique peptides, FDR < 1% and significance threshold $P <$ 0.05 (with 95% confidence). For protein quantification, the filters were set as follows: normalize with protein median and only unique peptides were used to quantify proteins.

A total number of 3376 proteins were identified with more than two unique peptides and < 1% global FDR in two biological replicates, among which 3237 proteins were quantified with CV < 10% (Supplementary Figure S5A and B). Basing on the null distribution of the 115/113 and

119/117 ratios and a type I error rate of 5%, cut-off values for up- and downregulated differential expression rate were determined to be 1.18 and 0.83, respectively (Supplementary Figure S5B).

High-throughput RNA sequencing

Total RNA from SSCs was isolated by TRIzol (Thermo Fisher Scientific). The RNA libraries were constructed by Illumina library preparation protocols. High-throughput sequencing was performed on HiSeq2000.

RNA sequencing analysis

For miRNA analysis, sequencing reads were mapped to the mouse genome (UCSC mm9) by Bowtie2 (v2.0.2). The reads of miRNAs were counted by bedtools coverage (V2.17.0). Reference miRNAs downloaded from miRBase (Release 21) were used for miRNA analysis. For mRNA analysis, data from sample duplicates were pooled for further analyses as correlation coefficients of gene expression levels from biological duplicates are all more than 0.95. The sequencing reads were mapped to the mouse genome (UCSC mm9) by TopHat (v2.0.6). The expression level of mRNAs was represented by FPKM calculated by Cufflinks (v2.0.2). The differentially expressed genes were identified with Cuffdiff based on the threshold of q-value being less than 0.05. RefSeq mRNAs downloaded from UCSC (mm9) were used as the reference mRNAs.

Gene ontology (GO) analysis

GO analysis was performed using DAVID bioinformatics tools (42). GO terms with $P < 1 \times 10^{-2}$ and enrichment score > 1.5 were considered significant.

Genomic PCR

We isolated genomic DNA as previous report (43) and carried out PCR using PrimeSTAR HS DNA Polymerase (Takara). See also Supplementary Table S6 for primer sequences.

Real-time PCR (qPCR)

Primers used in qPCR were listed in Supplementary Table S6. Total RNAs were isolated using TRIZol regent following the standard manufacture protocol. RNAs of 2 μg were reversed transcribed in 20 μl reaction system using random primers and the high-capacity cDNA Reverse Transcription Kit (Thermo Fisher Scientific). qPCR reactions were performed in the 96-plate format or 384-plate format of Roche LightCycler 480 real-time PCR system using the 2x Ultra-SYBR Mixture from Beijing CoWin Biotech. The data were analyzed using the comparative Ct method (ΔCt) with β-actin RNA as the internal control.

For quantification of miRNA, a strategy of poly(A)-tailed RT-PCR was used (44). RNAs of 2 μg were reversed transcribed by miRcute miRNA first-strand cDNA Synthesis kit from Tiangen, using specific adaptor primer. Real-time PCR reactions were carried out in the 96-plate format of Roche LightCycler 480 real-time PCR system, using miRcute miRNA qPCR detection kit (SYBR Green) from Tiangen. The data were analyzed using the comparative Ct method (ΔCt) with sno234 as the internal control.

Western blotting

SSCs under different conditions were washed with PBS and cell lysates were prepared using RIPA lysis buffer containing protease inhibitor cocktail (Roche). Samples containing 10 μg proteins were run in sodium dodecyl sulphate-polyacrylamide gel electrophoresis gel and transferred to nitrocellulose membranes (Whatman Protran). Membranes were then blocked in 5% nonfat-milk/PBST for 1 h, followed by incubation with the primary antibodies and HRP-conjugated secondary antibodies at room temperature for 4 h or at 4°C overnight with gently agitating. The proteins were detected using the Supersignal West Pico Chemiluminescent Substrate (Thermo Fisher Scientific) and then analyzed with the ChemiDoc XRS$^+$ system (Bio Rad).

Testis collection and histological analysis

Testes were collected immediately after the mice were sacrificed, fixed in 4% paraformaldehyde for up to 24 h and then dehydrated using gradient concentration of ethanol. After treated with xylene and embedded in paraffin, sections were prepared and mounted on APES-coated glass slides. After deparaffinization in xylene and re-hydration in gradient concentration of ethanol were performed, slides were stained with H&E for histological analysis or stained with antibodies for immunofluorescence using the following procedures.

Immunostaining and flow cytometry analysis

Cells or frozen sections were fixed in 4% paraformaldehyde and permeabilized with 0.1% Triton X-100. For immunofluorescence, after being incubated in 5% bovine serum albumin (BSA)/PBS, the samples were incubated with the primary antibodies and fluorophore conjugated secondary antibodies. Subsequently, samples were stained with DAPI (Sigma-Aldrich, 1 μg/ml). The images were captured by a laser confocal microscope (Leica). For immunohistochemistry, the sections were pretreated with 3% H_2O_2 and 5% BSA/PBS, followed by incubation with primary antibodies and HRP conjugated secondary antibodies. The sections were then stained with DAB and hematoxylin. The images were captured by a microscope equipped with a CCD camera (Nikon).

For flow cytometry analysis, after being incubated in 5% BSA/PBS, the cells were incubated with the primary antibodies and fluorophore conjugated secondary antibodies. The analyses were carried out on a CytoFLEX research cytometer (Beckman).

BrdU incorporation and TUNEL assay

For BrdU assays, Dox treated iKO-SC-1 or RA treated SSCs were further treated with 10 mg/ml BrdU (Sigma) for 12 h before cell were harvested. The cells were then collected, fixed with 70% ice-cold ethanol for 20 min at room

temperature. Then, the cells were denatured with fresh 2 M HCl and neutralized with 0.1 M sodium borate (pH 8.5). Then the cells were blocked in 5% BSA/PBS and incubated with mouse anti-BrdU antibody at 4°C overnight. Meanwhile, the control cells were incubated with mouse isotype IgG. The FITC-conjugated anti-mouse IgG was used as the secondary antibody. The cells were stained with DAPI and analyzed using Beckman flow cytometer.

For TUNEL assays, cells were collected and labeled using DeadEnd fluorometric TUNEL Symtem (Promega) following the standard protocol. Briefly, the cells were fixed with 4% paraformaldehyde followed by incubation with 70% ice-cold ethanol for 4 h at −20°C. After several washes, the cells were resuspended in Equilibration Buffer for 5 min at room temperature and then incubated with reaction buffer at 37°C for 1 h. Meanwhile, the control cells were incubated with buffer without the rTdT enzyme. The reaction was terminated with 20 mM ethylenediaminetetraacetic acid. The cells were stained with DAPI and analyzed using Beckman flow cytometer.

Dual luciferase assay

Luciferase constructs were produced as follows. 3′ UTRs for candidate genes were amplified from SSC cDNA and cloned into the pMIR-Report vector (Promega). Primers are listed in Supplementary Table S6.

HEK293FT cells were plated in a 96-well plate pretreated with 0.2% gelatin. Approximately 24 h later, microRNA mimics were first transfected using RNAiMAX. Ten hours later, 50 ng Firefly Luciferase report plasmids and 5 ng internal control plasmid expressing the Renilla Luciferase (pRL-TK, Promega) were co-transfected by Lipofectamine 2000 reagent (Life technologies). Cell extracts were prepared 24 h after transfection, and luciferase activity was measured using the Dual-Luciferase Reporter Assay System (Promega, USA) according to the manufacturer's protocol. Data were first normalized to empty vector then to mimics negative control-transfected 293FT.

Antibodies

Mouse antibody to Flag (F3165) was purchased from Sigma. Goat antibody to c-KIT (AF1356) was purchased from R&D. Rabbit antibody to MVH (ab13840) was purchased from Abcam. Rabbit antibody to RBFOX2 (A300-864A) was purchased from Bethyl Laboratories. Rabbit antibody to CPEB1 (13274-1-AP) was purchased from Proteintech. Mouse antibody to ACTB (M20010) was purchased from Abmart. Mouse antibody to BrdU (555627) was purchased from BD Pharmingen.

Statistical Analysis

Statistical analysis was conducted using the Student's *t*-test (two-tailed). All values are shown as mean ± SEM. $P < 0.05$ were considered statistically significant. One asterisk and two asterisks indicate $P < 0.05$, $P < 0.01$, respectively.

RESULTS

miR-202 is specifically expressed and dynamically regulated during mouse spermatogenesis

We previously profiled the dynamics of small RNAs of 18–36 nucleotides in type A spermatogonia (SG-A), pachytene spermatocytes (pacSC) and round spermatids (rST) (33). In the present study, we re-analyzed this data set (GSE24822) to examine the expression of miRNAs in more details. A miRNA was considered to be actively transcribed if its cloning frequency (CF), which is its percent read count value divided by all read counts in a sample, to be > 0.01% (32). Based on this CF cutoff, 307 miRNAs were found to be expressed in at least one of the 3 spermatogenic cell types, and were named g-miRNAs for germ cell-expressed miRNAs (Supplementary Table S1, Supplementary Figure S1). The expression dynamics of g-miRNAs in SG-A, pacSC and rST and several other organs were shown by the heat map of the hierarchical clustering analysis (Figure 1A). We also identified 67 miRNAs specifically expressed in the mouse testis (Supplementary Table S2) based on the small RNA multi-organ expression data set (GSE21630) generated by Kuchen *et al.* (34) using a tissue-specificity evaluation algorithm (Testis JS-score > 0.5) proposed by Cabili *et al.* (45).

Based on miRNA abundances in SG-A, miR-202-5p ranks the 4th following three let-7 family members (CF = 7%, Supplementary Table S1). Moreover, miR-202-3p and miR-202-5p are among the 67 testis-specific miRNAs (Supplementary Table S2). Using qRT-PCR, we confirmed that the abundances of miR-202-3p and miR-202-5p were indeed much higher in the testis than in any of the other tissues examined by several orders of magnitude (Figure 1B). Based on the standard expression curves made using synthetic miRNAs (Figure 1C), we found that miR-202-3p and miR-202-5p were expressed at similar levels in SSCs, and the level of miR-202-5p was about 75% of that of miR-202-3p. However, their levels in other spermatogenic cell types are different and change in opposite ways during spermatogenesis (Figure 1D, Supplementary Figure S1). Previously, Niu *et al.* (32) reported that miR-202-5p was more abundantly expressed in $Thy1^-$ somatic cells (Sertoli and Leydig cells) than in $Thy1^+$ SG-A, and our results using the primary culture of Sertoli cells confirmed this observation. Moreover, we found that miR-202-3p was upregulated by GDNF and downregulated by RA while miR-202-5p was up-regulated by RA (Figure 1E). These results suggested that transcripts of miR-202, particularly miR-202-3p, might play an important role in SSCs during spermatogenesis.

Inhibition of miR-202-3p but not miR-202-5p induces differentiation of SSCs

To test whether miR-202-3p and/or miR-202-5p indeed play a role in SSCs, we treated feeder-free SSC cultures with Cy3-labeled synthetic oligonucleotide inhibitors that target these two miRNAs. The inhibitor was introduced into SSCs by lipofectamine transfection, and more than 90% of the cells were transfected as indicated by Cy3 fluorescence when checked 2 days after transfection (Supplementary Figure S2A). Four days upon transfection with miR-202-3p

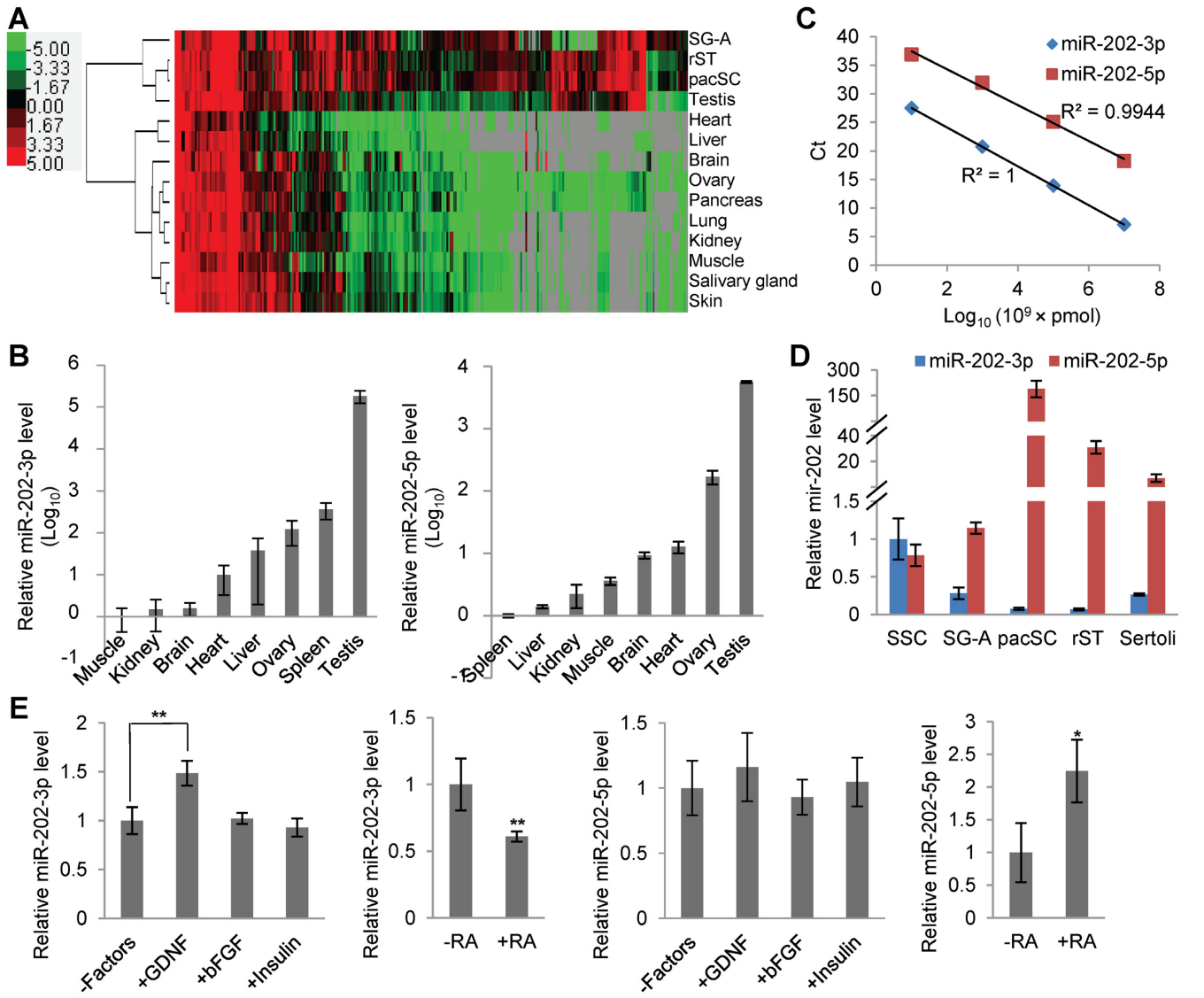

Figure 1. Expression and regulation of miR-202-3p and miR-202-5p. (**A**) Clustering analysis of miRNAs highly expressed in at least one of the three spermatogenic cell types of SG-A, pacSC and rST. The values of the heat map are Log_2 (CFs ×10 000). (**B**) qPCR analyses of miR-202-3p and miR-202-5p in multiple organs. (**C**) Standard expression curves of miR-202-3p and miR-202-5p plotted as Ct values verse the concentrations of miRNAs. (**D**) qPCR analyses of miR-202-3p and miR-202-5p in spermatogenic cells. (**E**) Regulation of miR-202-3p and miR-202-5p by growth factors and RA determined by qPCR. n = 4 for miR-202-3p and n = 3 for miR-202-5p.

inhibitor, flat patches of SSCs with clear cell boundaries, typical of differentiating spermatogonia, were observed in sharp contrast to the tight clumps of SSCs without inhibitor treatment or treated with the control inhibitor of scrambled sequence (Figure 2A, Supplementary Figure S2B). At this time, while the number of SSCs of the scramble control was not significantly different from that of the mock control, the number of SSCs treated with the inhibitor was reduced to about 76% of the value of the mock control (Figure 2B). In contrast, treatment of SSCs with miR-202-5p inhibitors brought forth no changes in either the morphology or the number of SSCs (Figure 2A and B). The induced differentiation of SSCs by miR-202-3p inhibitor was supported by the reduced expression of *Plzf*, and the elevated expression of *Stra8*, *Dazl* and *Sycp3* as detected by qRT-PCRs (Figure 2C).

As a result of differentiation, the number of stem cells in the SSC culture was also expected to decrease. To test this, SSCs were first infected with the EGFP-expressing lentivirus to become green fluorescent SSCs (EGFP-SSCs), then treated with either the miR-202-3P specific inhibitor or the scramble control inhibitor for 4 days, and subsequently transplanted into the testes of busulfan-pretreated recipient mice (Figure 2D). Two months later, the recipient testes were harvested for EGFP-colony counting, and we found that the miR-202-3p specific inhibitor but not the scramble control reduced the stem cell activity by 75% when compared with the mock control (Figure 2E). These results

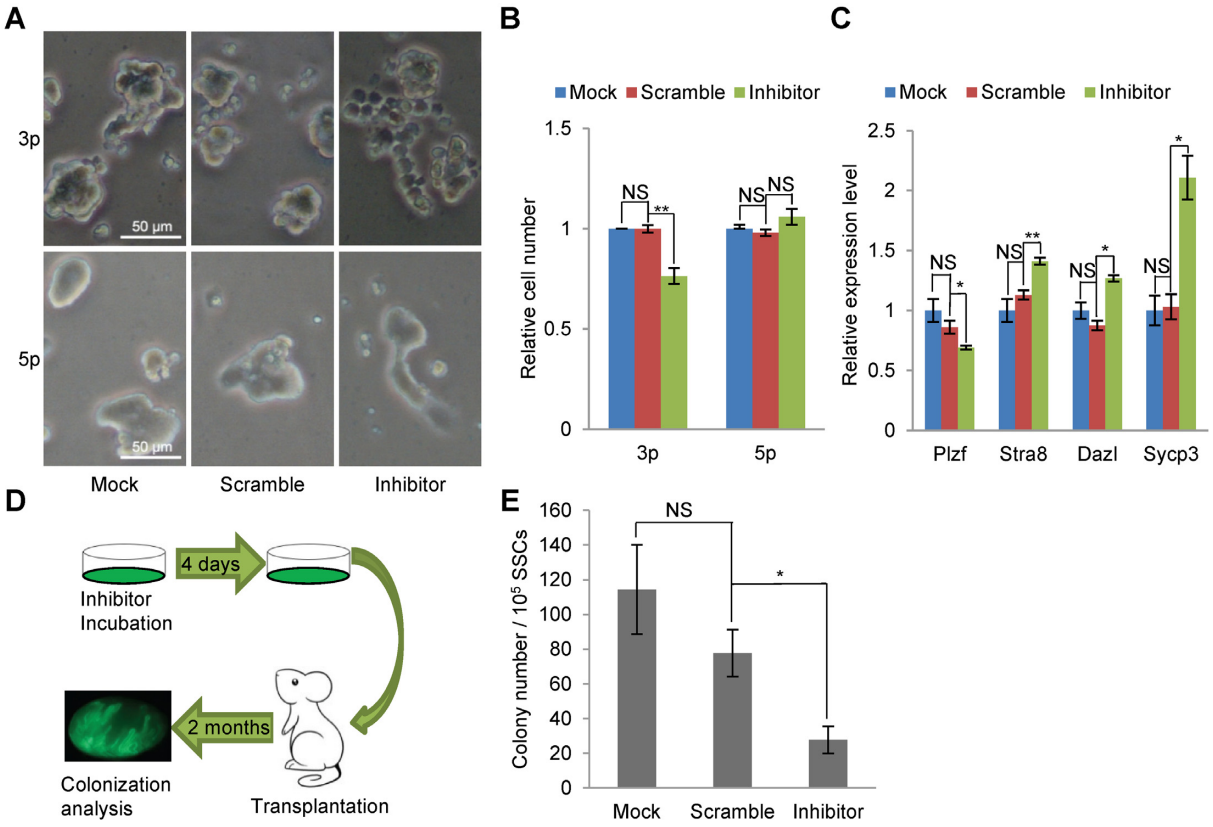

Figure 2. Inhibition of miR-202-3p induces differentiation of SSCs. (**A**) Bright field images of SSCs treated with inhibitors for miR-202-3p and miR-202-5p on day 4 of treatment. (**B**) Quantification of cell numbers of feeder-free SSCs on day 4 of treatment with inhibitors. n = 5 for miR-202-3p and n = 3 for miR-202-5p. Data are normalized to mock SSCs. (**C**) qPCR analysis of the expression of marker genes in SSCs on day 4 of treatment with miR-202-3p inhibitor (n = 3). (**D**) The scheme of transplantation assays for assessing the stem cell contents of cultured SSCs. (**E**) Quantitative results of stem cell content assessment of SSCs treated with miR-202-3p inhibitor and controls by following the scheme in (D) (n = 3).

show that miR-202-3p blocks the differentiation of SSCs and sustains their stem cell identity *in vitro*.

Knockout of miR-202 induces differentiation of SSCs to c-KIT$^+$ spermatogonia

We next set out to study the function of miR-202 by knocking out its gene in SSCs using the CRISPR-Cas9 system. We first derived an iCas9-SSC line using a lentiviral vector, from which the expression of Cas9 can be induced by Dox treatment. The integration of the Cas9 cassette into the genome was confirmed by genomic PCR and its Dox-induced expression was validated by Western blotting (Figure 3A and B). The validity of this inducible CRISPR-Cas9 system was further confirmed by the reduced fluorescence of the EGFP-SSCs after a lentiviral construct expressing the EGFP-specific gRNA was introduced to the cells followed by Dox treatment for 4 days (Supplementary Figure S3).

We designed a pair of gRNAs to knockout miR-202. The double gRNAs were expressed in one lentiviral plasmid construct under two independent U6 promoters (Figure 3C). Control plasmid containing scrambled DNA sequences of gRNAs were similarly constructed. As the constructs also contains an EGFP-expressing cassette, green fluorescent cells were derived, expanded and purified by FACS to derive the iKO-SSCs and Ctr-iKO-SSCs, respectively, upon lentiviral infection of iCas9-SSCs (Supplementary Figure S4A). The cells of these two lines grew as tight clumps under normal culture condition. The KO of miR-202 was confirmed by the detection of a truncated genomic fragment in addition to the wild type one using PCR assays (Figure 3D). As SSCs can proliferate without feeder cells for a short period of time, we also performed KO experiments under the feeder free condition to examine the effect of miR-202 KO. At day 4 of Dox treatment, the number of iKO-SSCs was reduced by 60% compared with cells without treatment regardless of the use of MEF feeder cells or not. In contrast, the same treatment had no effect on the number of Ctr-iKO-SSCs (Figure 3E). It was noteworthy that the cell number reduction was not significant on day 2 of treatment (Figure 3F). Similar results were acquired when we used a second pair of gRNAs to knock out miR-202 (iKO-SSCs-2) (Figure 3E). To show that the phenotypes of iKO-SSCs would be rescued by the expression of exogenous miR-202, we developed an independent cell line (iKO-OE-SSCs), into which the gRNA expression construct containing an additional U6-miR-202 cassette was introduced. For this cell line, Dox treatment did not reduce the cell number significantly (Supplementary Figure S4B).

We further investigated the effects of miR-202 KO by using SSC clones expanded from single cells. Twenty-six (iKO-SC-1∼26) and 7 (Ctr-SC-1∼7) clones were developed

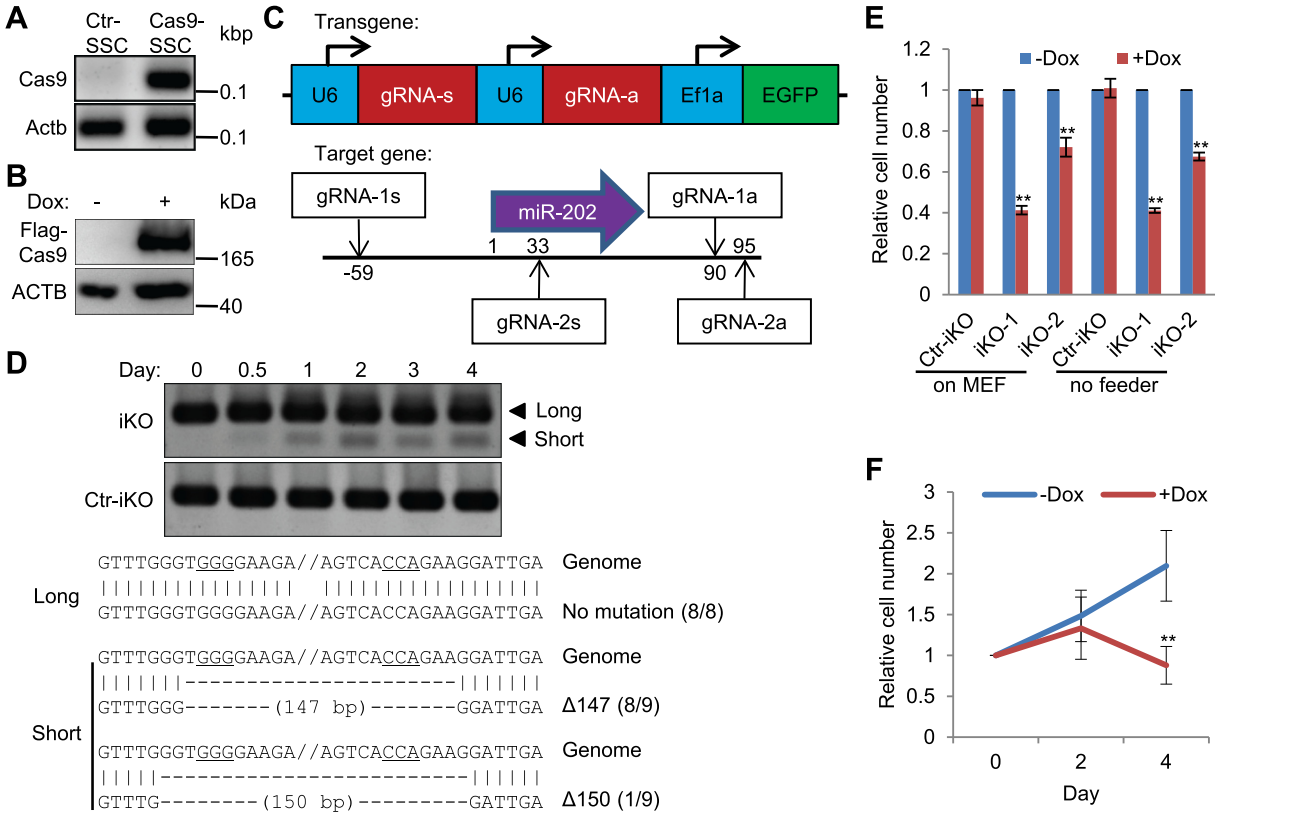

Figure 3. Deletion of miR-202 using inducible CRISPR-Cas9 system reduces the proliferation of SSCs. (**A**) PCR detection of Cas9 sequence integrated in the genome of SSCs. (**B**) Western blotting detection of Flag-Cas9 induced by Dox treatment. (**C**) Schematic illustration of gRNA expression from the lentiviral vector and their target sites in the genome. (**D**) Detection of miR-202-deleted genomic sequence in Doxycycline-treated iKO-SSCs and Ctr-iKO-SSCs by PCRs and sequencing. PAM sites are underlined. (**E**) Quantification of cell numbers of Ctr-iKO-SSCs, iKO-SSCs and iKO-SSCs-2 on day 4 of treatment. n = 5 for Ctr-iKO-SSCs (Ctr-iKO) and iKO-SSCs (iKO-1); n = 3 for iKO-SSCs-2 (iKO-2). (**F**) Time course of cell number changes of iKO-SSCs with and without Dox treatment. Data are normalized to the value on day 0 of treatment (n = 3).

from iKO-SSCs and Ctr-iKO-SSCs, respectively (Supplementary Figure S4C and D). Majority of the clones from iKO-SSCs reduced their cell number in response to Dox at day 4 of treatment while none of the clones from Ctr-iKO-SSCs changed their cell numbers (Supplementary Figure S4D). Clones iKO-SC-1, 2, 3 and 4 and Ctr-iKO-SC-1 and 2 were selected for further study. iKO-SC-1∼4, when treated with Dox, all reduced their cell numbers by more than 70% regardless whether they were cultured on MEF feeder layers or not (Figure 4A). Again, we introduced the U6-miR-202 cassette into the cells of iKO-SC-1, 2 and 3 by lentiviral infection (Figure 4B) and found that the cell number reduction of these clones in response to Dox treatment were significantly reverted by the ectopic expression of miR-202 (Figure 4C), suggesting that the phenotypes of miR-202 KO SSCs were a direct consequence of the deletion of the miR-202 gene.

We further assessed the effects of miR-202 KO by examining the expression changes of a panel of marker genes that are specifically expressed in either undifferentiated/differentiating spermatogonia or spermatocytes. Dox treatment of iKO-SC-1 for 2 days reduced miR-202-3p expression by about 80% (Figure 4D). At this time point, the expression of maker genes for undifferentiated SG (*Oct4*, *Lin28a*, *Gfra1*, *Plzf* and *Nanos3*) decreased, while the expression of marker genes for differentiating SG (*c-Kit*) and meiotic SC marker genes (*Sycp3*, *Prdm9* and *Dmc1*) increased (Figure 4D). Moreover, the generation of differentiating SG was further demonstrated by the positive immunostaining of the c-KIT protein (Figure 4E). Markedly, the percentage of c-KIT$^+$ cells increased from 5% to 56% when miR-202 was knocked out as quantified by the FACS analysis (Figure 4F and G). These results showed that the induced KO of miR-202 resulted in compromised proliferation and differentiation of SSCs.

Knockout of miR-202 reduces stem cell activity of SSCs

We next examined whether KO of miR-202 changes the stem cell activity of SSCs using transplantation experiments. Cultured iKO-SSCs and Ctr-iKO-SSCs were transplanted into the testes of busulfan-pretreated mice. Four weeks later, recipient mice were fed with drinking water containing 2 mg/ml Dox. Six weeks after treatment, recipient mice were sacrificed and their testes were examined (Figure 5A). Testes transplanted with SSCs of iKO-SSCs (iKO-testes) were 40% smaller than those transplanted with Ctr-iKO-SSCs (Ctr-testes) on average (Figure 5B and C). Histological examination of testes showed that the iKO-testes contained many germ cell-depleted tubules while the Ctr-testes contained only normal-looking tubules (Figure

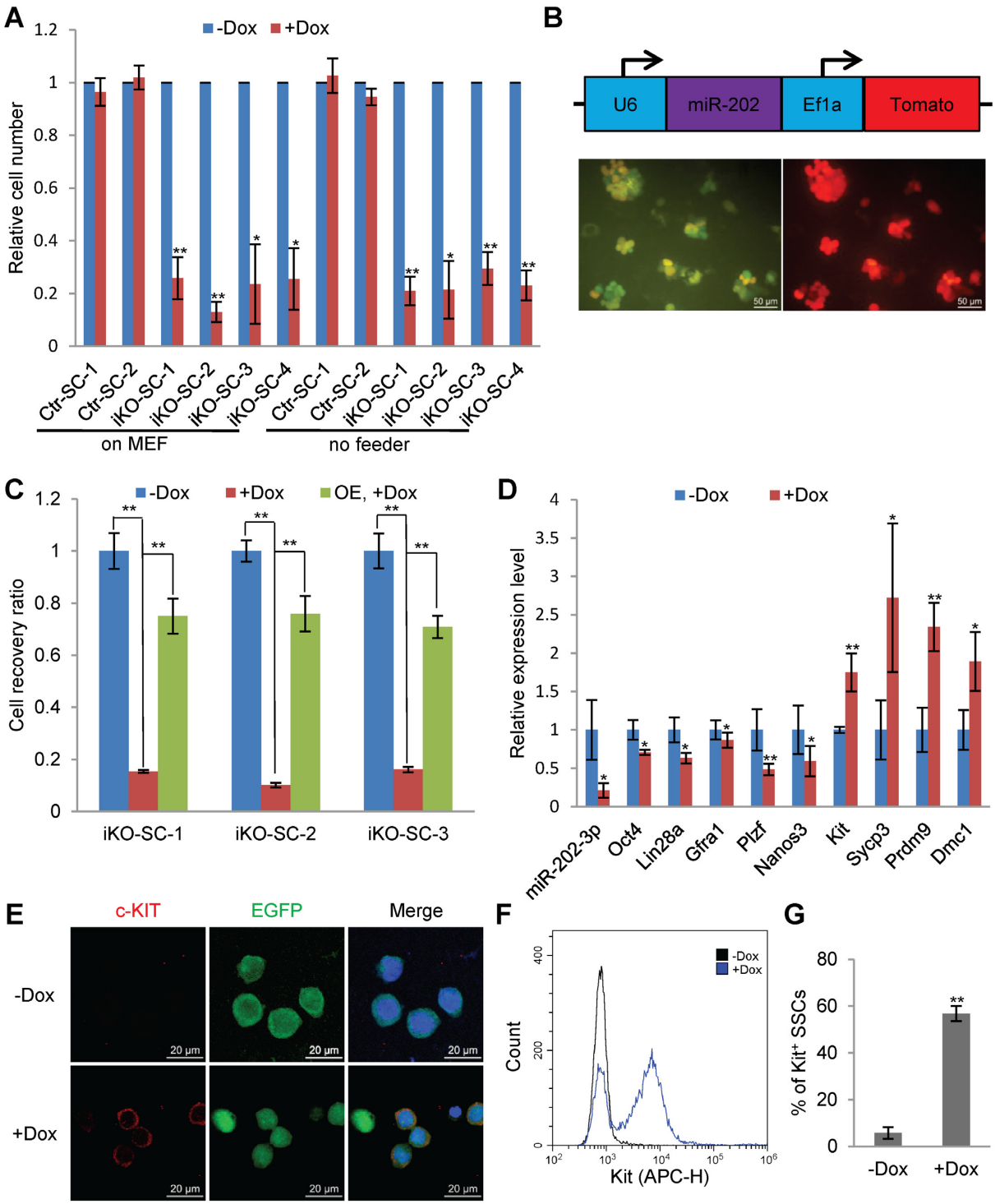

Figure 4. Reduced proliferation of and the generation of c-KIT$^+$ spermatogonia from miR-202-KO SSCs expanded from single cells. (**A**) Quantitative analyses of the proliferation of SSC clones expanded from single cells of iKO-SSCs (iKO-SC-1-4) and Ctr-iKO-SSCs (Ctr-iKO-SC-1-2). Data are normalized to SSCs without induction (n = 4). (**B**) Ectopic expression of miR-202 in SSCs of clone iKO-SC-1-3. Upper panel, the structure of the expression cassette; lower panel, fluorescent images of cells, which express EGFP from the double gRNA construct (see also Figure 3C) and Tomato from the ectopic expression construct. (**C**) Rescue of proliferation changes of SSCs in response to Dox treatment by the ectopic expression of miR-202 in clones iKO-SC-1-3. Data are normalized to SSCs without Dox treatment (n = 3). (**D**) qPCR analysis of marker gene expression on day 2 of Dox treatment (n = 3). (**E**) Immunofluorescence of c-KIT in cells on day 2 of Dox treatment. Blue color is from DAPI staining. (**F**) A representative plot of flow cytometry analysis of c-KIT$^+$ cells on day 2 of Dox treatment. (**G**) Quantitative results of flow cytometry analyses of c-KIT$^+$ SSCs represented by (E) (n = 3).

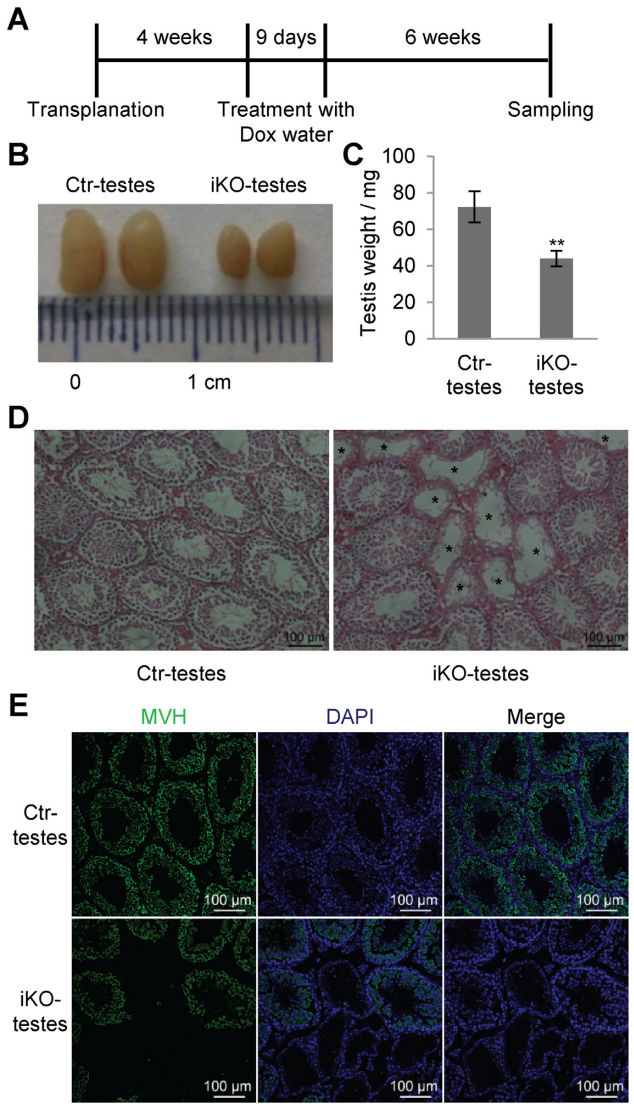

Figure 5. Stem cell activity assessment of SSCs by transplantation assays. (**A**) The scheme of transplantation assay for Ctr-iKO-SSCs and iKO-SSCs. (**B**) Images of Ctr-testes and iKO-testes. (**C**) Testis weight of Ctr-testes and iKO-testes after Dox treatment (n = 5). (**D**) Hematoxylin and Eosin (HE) images of testicular sections of Ctr-testes and iKO-testes after Dox induction. Germ cell-depleted tubules of iKO-testes are marked by asterisks. (**E**) MVH immunostaining of sections from Ctr-testes and iKO-testes to show the germ cell changes in response to miR-202 KO induced by Dox treatment. Paraffin sections of 5 μm were analyzed by immunofluorescence.

5D). The presence/absence of germ cells in the seminiferous tubules of transplanted testes were further demonstrated by the positive immunostaining results of MVH, a specific marker for germ cells from SSCs to early round spermatids (Figure 5E). In summary, induced knockout of miR-202 reduced the stem cell activity of cultured SSCs.

Screening of miR-202 targets by differential proteomic analysis and RNA sequencing

We set out to screen for targets of miR-202 by identifying proteins that change their expression in response to miR-202 KO using the iTRAQ-based proteomic approach. As the protein changes of true targets would likely be reversed by the ectopic expression of miR-202, we included in our analyses cells of iKO-SC-1, iKO-SC-2, as well as two samples of iKO-OE-SSCs with and without Dox treatment. Consequently, a total of 8 protein samples were labeled with 8 different isotopic agents simultaneously and were subjected to LS/MS analyses (Figure 6A). As a result, 118 proteins were found to change their abundances in response to miR-202 KO, while only 29 differential proteins were identified between the two samples of iKO-OE-SSCs, and the intersection of these two sets was just 2 (Figure 6A, Supplementary Table S3). These results indicated that the abundance changes of most proteins in response to Dox treatment were most likely a direct result of miR-202 KO instead of the off-target effects of the CRISPR-Cas9 system.

We further used dual luciferase assay to validate a selected panel of potential miR-202 targets including *Rbfox2*, *Cpeb1*, *Syncrip*, *Ercc2*, *Nid2*, *Mtmr12* and *Nras*, which increased their protein levels in response to miR-202 KO and which are also predicted targets of miR-202-3p. *Rbfox2*, *Cpeb1* and *Syncrip* are RNA binding protein genes; the *Ercc2* protein is involved in transcription-coupled nucleotide excision repair; *Nid2* encodes a member of the nidogen family of basement membrane proteins; the protein encoded by *Mtmr12* is an adapter subunit in a complex that contains a PtdIns(3)P 3-phosphatase; NRAS has GTPase activity involved in multiple processes such as cell cycle control. Therefore, these genes represent different genes families enriched in the miR-202 target gene set. The predicted target sequences in 3′ UTRs of *Rbfox2*, *Cpeb1*, *Ercc2* and *Nid2* but not the ones of *Syncrip*, *Mtmr12* and *Nras* reduced luciferase activity of the fusion genes in response to miR-202 mimic treatment (Figure 6B). As negative controls, none of the mutated target sequences had any effect on the luciferase activity. Therefore, *Rbfox2*, *Cpeb1*, *Ercc2*, *Nid2* were direct targets of miR-202. As the iTRAQ proteomic assay may not be sensitive enough to detect all targets of miR-202, we identified additional ones by bioinformatics predictions. We showed that the predicted target Cpeb3 was also a direct target (Figure 6B).

As miRNAs regulate gene expression either by inhibiting translation or by initiating mRNA degradation, we performed RNA sequencing to identify more genes regulated by miR-202 (Supplementary Table S4). Consequently, 148 and 7 genes were up- and downregulated in response to miR-202 KO. The upregulated set detected by RNA sequencing overlap that detected by proteomic analyses by 14 genes while the two downregulated sets had no overlap (Figure 6C). Markedly, the upregulated proteins and mRNAs share many enriched GO terms such as M phase, cell cycle, mitosis, microtubule-based process, cytoskeleton organization. The upregulated proteins are also enriched with terms such as meiosis, RNA processing while the upregulated mRNAs are enriched with terms such as cell death and apoptosis (Figure 6D, Supplementary Table S5). In contrast, the downregulated sets are not enriched with any GO terms. Therefore, miR-202 seems to mainly regulate genes involved in mitotic division either by inhibiting their translation or by inducing their mRNAs to degrade.

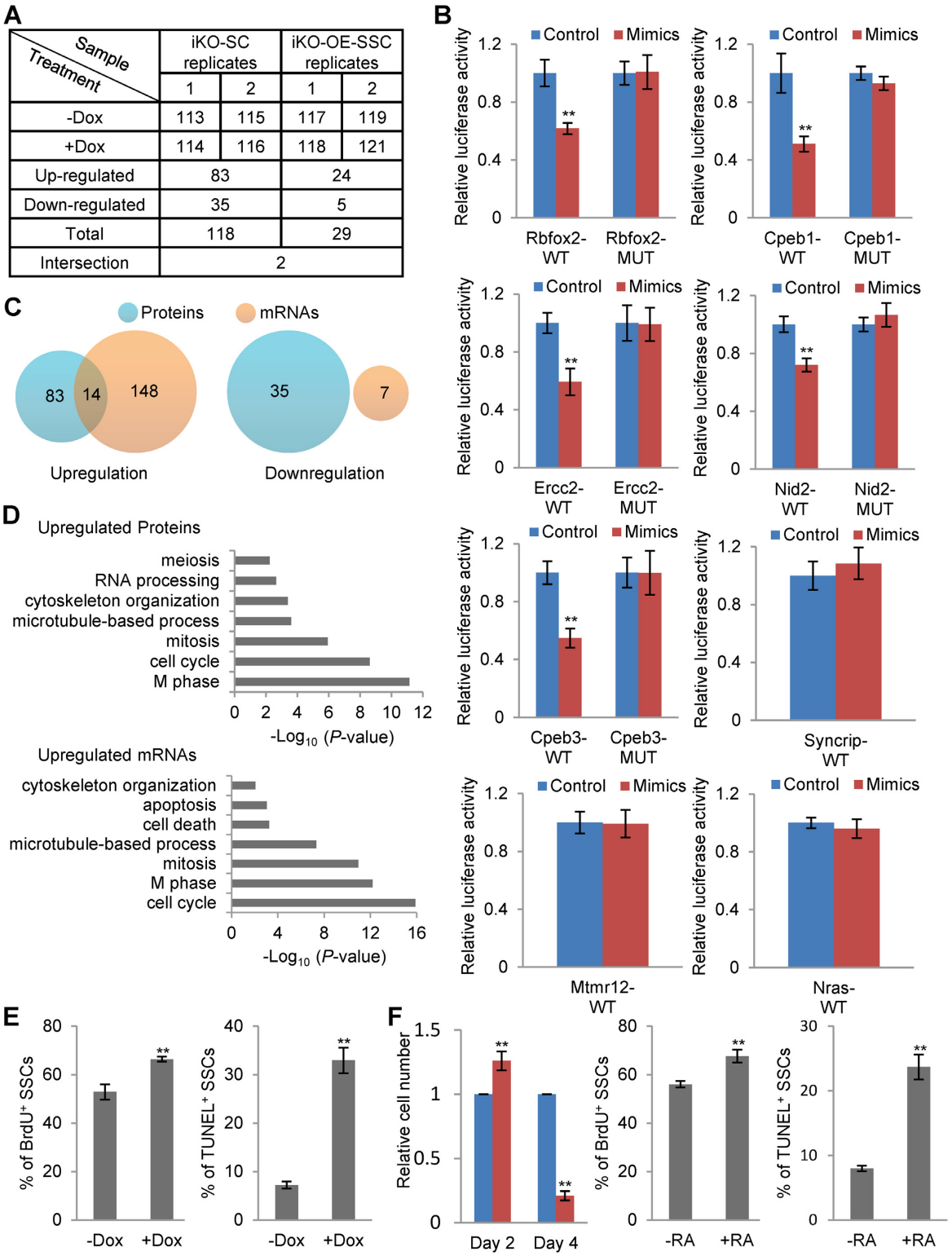

Figure 6. Proteomic and transcriptomic analyses of targets of miR-202. (**A**) The scheme of sample preparation for the differential proteomic analyses and the numbers of up- and downregulated proteins in response to miR-202 KO. The number 113–119, and 121 represent the isotopes used to label protein samples in the iTRAQ experiments. (**B**) Validation of proteomic approach-identified targets of miR-202 by dual luciferase assays (n = 6). (**C**) Venn diagrams showing the overlaps between up-/downregulated genes in response to miR-202 KO identified using proteomic and transcriptomic analyses. (**D**) GO terms enriched in upregulated gene sets. (**E**) BrdU incorporation and TUNEL assays of Dox-treated iKO-SC-1 by flow cytometry analyses on day 2 of treatment (n = 5 for BrdU and n = 4 for TUNEL). (**F**) Assessment of cell proliferation (n = 4), mitotic division (n = 5) and apoptosis (n = 4) of RA-treated SSCs on day 2 of treatment.

miR-202 is a negative regulator of cell cycle in SSCs

Based on these proteomic and transcriptomic screening results, miR-202 is likely a suppressor for the mitotic division of differentiating spermatogonia. To resolve this seeming contradiction to the observed decrease in total cell number induced by miR-202 KO, we examined the changes in mitotic activity and apoptosis of SSCs in response to miR-202 KO using BrdU incorporation and TUNEL assays. Dox treatment of iKO-SSC-1 cells for 2 days increased the percentage of $BrdU^+$ cells from 53% to 66% and the percentage of apoptotic cells from 7% to 33% (Figure 6E, Supplementary Figure S5C). Therefore, miR-202 KO resulted in a bigger increase of apoptotic cells than mitotic cells and this explained the significant reduction of total cell number on day 4. Our previous work showed that RA induced differentiation and meiosis initiation of SSCs accompanied by increased apoptosis (4). Here, we found that RA treatment also increased the percentage of $BrdU^+$ cells although to a less degree (from 56% to 68%) compared with the increase in apoptotic cells (from 8% to 24%), resulting in a decrease in the total cell number on day 4 of treatment (Figure 6F, Supplementary Figure S5D). These results showed that KO of miR-202 speeded up the cell cycle and incurred a larger degree of apoptosis of differentiating spermatogonia in a similar manner to RA treatment.

The miR-202 target *Rbfox2* is essential for meiosis initiation

As many RNA binding proteins have essential roles in spermatogenesis, we next selected *Rbfox2* and *Cpeb1* to investigate how the function of miR-202 was mediated by its direct target genes. The translational inhibition of *Rbfox2* and *Cpeb1* was first confirmed by Western blotting analysis using the iKO-SC-1 cells treated with Dox for 2 days (Figure 7A). qRT-PCR results showed that both *Rbfox2* and *Cpeb1* increased their mRNA levels markedly when meiosis is initiated in preleptotene spermatocytes (Figure 7B), in sharp contrast to the change pattern of miR-202-3p (Figure 1D). Immunostaining of these two proteins also confirmed their higher abundance in pacSC than in the earlier stages of pacSC (Figure 7C).

Pretreatment of iKO-SC-1 cells with siRNAs of *Rbfox2* and *Cpeb1* 6 h before Dox treatment resulted in a cell number reduction to a smaller degree compared with cells pretreated with siRNAs of scrambled sequences (Figure 7D, Supplementary Figure S6). Therefore, the reduced proliferation of miR-202 KO SSCs was partially rescued by the knockdown of its targets *Rbfox2* and *Cpeb1*.

We further examine the function of these two genes using shRNAs expressed from an EGFP-expressing lentiviral construct, which is transferred into the cells by viral infection. Based on our meiosis initiation model recently established, SSCs were cultured on Sertoli cells and treated with RA, and the initiation of meiosis was determined by observing the immunostaining of SYCP3 (4). As the viral infection is not 100%, those uninfected $EGFP^-$ cells were mostly $SYCP3^+$ while those $EGFP^+$ cells, in which *Rbfox2* was knocked down, were all $SYCP3^-$. In contrast, most of the $EGFP^+$ cells, in which *Cpeb1* was knocked down, were also $SYCP3^+$ (Figure 7E). These results indicate that *Rbfox2* but not *Cpeb1* plays an important role in the initiation of meiosis.

DISCUSSION

The essential roles of miRNAs in mammalian spermatogenesis are mainly inferred from the infertile phenotypes of gene KO mice of key enzymes for miRNA biogenesis, and the functions of most of individual miRNAs remain unknown. In the present study, we have identified a set of miRNAs highly or specifically expressed spermatogenic cells by analyzing small RNA sequencing data previously published (Supplementary Table S1). We selected miR-202 for further functional studies because of its much higher level expression in the testis compared with other organs and its regulation by GDNF and RA. Applying an inducible CRISPR-Cas9 KO technique to cultured SSCs, we showed that miR-202 played a role in maintaining the stem cell pool of SSCs by blocking their premature differentiation, which is typical of faster cell cycle and increased apoptosis. Using a differential proteomic approach and RNA sequencing, we screened out a large number of potential target genes of miR-202 including cell cycle regulators and RNA binding proteins. We used our *in vitro* meiosis model recently reported to further study the function of two direct targets, *Rbfox2* and *Cpeb1*, and found that *Rbfox2* but not *Cpeb1* was essential for meiosis initiation. Based on these results, we have identified a SSC fate decision regulatory network, through which miR-202 relays signals from paracrine factor GDNF and para/autocrine factor RA to a large number of downstream effectors including cell cycle regulators and RNA binding proteins (Figure 7F).

The miR-202 gene and its two mature transcripts have the following interesting features. First, both miR-202-3p and miR-202-5p are expressed in the testis at a much higher level than in any other tissues examined. miR-202-3p is expressed in the testis 600-fold higher than in the spleen, in which it is the second most abundant, while miR-202-5p in the testis is 30-fold higher than in the ovary (Figure 1B). Second, miR-202-3p and -5p change their expression pattern in opposite ways although their abundances in SSCs are comparable, suggesting that they may have different roles in spermatogenesis. While miR-202-3p is most abundant in SSCs and least abundant in pacSC, miR-202-5p is most abundant in pacSC, 200-fold higher than in SSCs (Figure 1D). Third, miR-202-3p was upregulated by GDNF and downregulated by RA while miR-202-5p was only upregulated by RA (Figure 1E). Fourth, miR-202-3p but not miR-202-5p acts as gatekeeper of SSC differentiation. The mechanism underlying the dynamic changes of these two miRNAs and the function of miR-202-5p at other stages of spermatogenesis warrant further investigations.

That miR-202 acts as a stem cell gatekeeper is reminiscent of the functions of several other miRNAs that are highly expressed in early stage spermatogenic cells. For example, based on our analysis (Supplementary Table S1), 8 members of the let-7 family, 2 members of the miR-30 family and miR-125a-5p are all most abundantly expressed in SG-A compared with pacSC and rST. These miRNAs increase their expression levels from early PGCs to late stage male PGCs when mitotic arrest occurs (7). The let-7 fam-

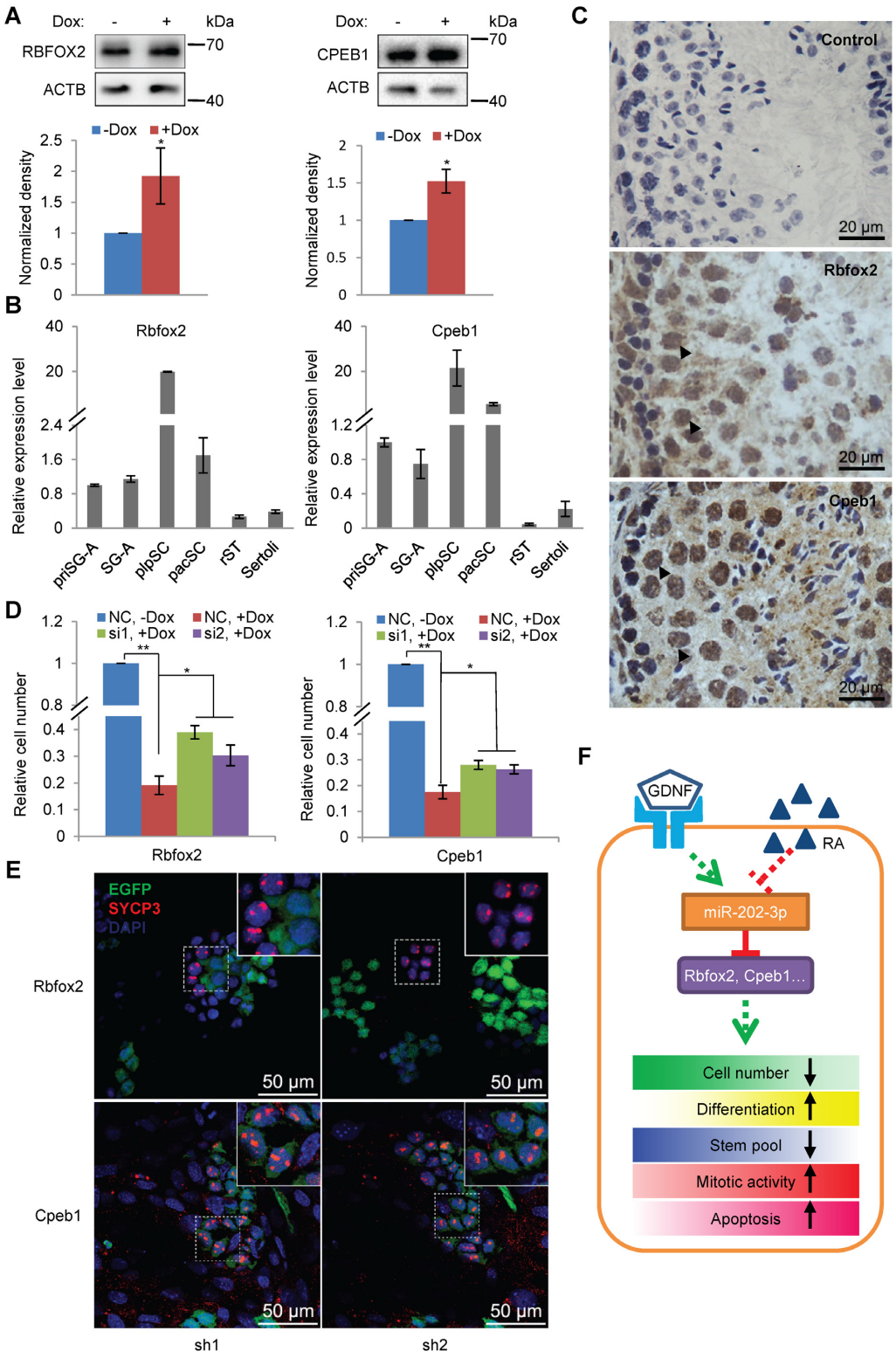

Figure 7. The miR-202 target Rbfox2 is essential for meiosis initiation. (**A**) RBFOX2 and CPEB1 increased their protein levels in response to miR-202 KO induced by Dox treatment (n = 3 for RBFOX2 and n = 4 for CPEB1). (**B**) qPCR analyses of *Rbfox2* and *Cpeb1* expression in different germ cell types. Data are normalized by the value of priSG-A (primitive SG-A) (n = 3). (**C**) Immunostaining of RBFOX2 and CPEB1 in mouse testis. Frozen sections of 10 μm were analyzed by immunohistochemistry. Arrowheads indicate pacSC with strong signals. (**D**) Proliferation assessment of iKO-SC-1 cells with and without the knockdown of *Rbfox2* and *Cpeb1* on day 4 of Dox treatment (n = 3 for *Rbfox2* and n = 4 for *Cpeb1*). (**E**) Evaluation of meiosis initiation of SSCs by EGFP immunofluorescence and SYCP3 immunostaining. Insects are enlarged images of $SYCP3^{+}$ SSCs. (**F**) A schematic model of a regulatory network that regulates the fate of SSCs in response to GDNF and RA. The signals were transduced to many effectors such *Rbfox2* and *Cpeb1* by miR-202 to change the proliferation, differentiation, stem cell activity, mitotic division and apoptosis.

ily members and miR-125a repress *Lin28*, a key controller of stem cell pluripotency, which is also implicated in the establishment of testicular teratomas, and have been recognized as tumor suppressors (46). The antagonistic interaction between the let-7 miRNAs and *Lin28* in spermatogonia has been confirmed (17). Using *in vitro* assays, miR-21, miR-20, miR-106a, miR-146, miR-221/222 have been shown to be important in maintaining the stem cell population (18–20,32). However, these studies only use miRNA mimics and/or inhibitors to investigate the roles these miRNAs and lack in-depth mechanistic explanations. No study on the function of miR-202 in spermatogenesis has been conducted so far and only several recent studies show that it acts as a tumor suppressor gene (47,48). It is downregulated in tumor cells and its overexpression suppresses cell proliferation and tumorigenicity. It targets some genes involved in cell cycle promotion, and is activated by p53 family members including, p53, p63 and p73 (49). In the present study, we not only established the essential role of miR-202 in SSC maintenance using an inducible CRISPR-Cas9 but also identified a large number of potential targets using proteomic and transcriptomic methods.

Our proteomic and transcriptomic data consistently show that miR-202 targets the mRNAs of many cell cycle regulators. Cell population amplification in many developmental processes is mainly carried out by transit differentiating cells and/or progenitors cells, which are primed for terminal differentiation. Adult stem cells are believed to be in a relative inert state because their over-activation is a major cause of tumorigenesis (50). Spermatogenesis is highly productive due to the active mitotic division of spermatogonia. A subset of the $PLZF^+$ undifferentiated spermatogonia are believed in a quiescent state (51,52). Based on the *in vivo* phenotypes of their gene KO mice, several protein-coding genes, including *Plzf* (52), *Nanos2* (51), *Tsc22d3* (53), *Dnmt3l* (54), have been reported to be essential in maintaining the quiescent state of SSCs. SSCs in culture finish a mitotic cell cycle in about 2.5–5.6 days, much slower than ESCs (55,56). However, their mitotic activity has not been compared with other types of spermatogonia. In the present study, we showed that the c-KIT^+ differentiating spermatogonia induced either by miR-202 gene KO or by RA have a higher mitotic activity compared with the normally cultured SSCs. Despite of the enhanced mitosis, both these two types of induced differentiation are not as productive as the *in vivo* one partially due to the increased apoptosis, and the net result of these two opposing processes is the decrease of the total cell number. Nevertheless, our work added miR-202 to the list of stem cell gatekeepers as a new member from the miRNA family.

It is not surprising that many targets of miR-202 are RNA binding proteins (RBPs) as RBPs such as DAZL, MVH, LIN28 play important roles in spermatogenesis. We selected two RBPs, RBFOX2 and CPEB1, to validate their regulation by miR-202 and to study their function in spermatogenesis. RBFOX2 is one of the three mammalian BBFOX family members, which are evolutionarily conserved regulators of tissue-specific alternative splicing in metazoa. The function of *Rbfox2* in spermatogenesis has not been elucidated. CPEB1 is one of the four mammalian paralog proteins that regulates the stability and translation of target mRNAs. When *Cpeb1* is knocked out, the female mice are completely infertile while the male mice impair their fertility severely, and all mice arrest their gametogenesis at the pachytene stage of the meiosis (57). *Sycp1* and *Sycp3* have been identified as the direct targets of CPEB1. We find that both *Rbfox2* and *Cpeb1* are direct targets of miR-202 as supported by the following lines of evidence: (i) Their proteins levels were elevated in response to miR-202 KO as detected by both proteomic and Western blotting analyses; (ii) Their targeting by miR-202 was confirmed by dual luciferase assays; (iii) The mRNA expression patterns of these two proteins are negatively correlated with that of miR-202-3p; (iv) The reduction of cell number caused by miR-202 KO can be partially rescued by the knockdown of these two genes. Using our *in vitro* meiosis model, we found that *Rbfox2* was essential for meiosis initiation while *Cpeb1* was not, and this is consistent with the observation that *Cpeb1* KO mice arrested spermatogenesis at the pachytene spermatocyte stage. Therefore, miR-202 represses the genes that execute their functions at different stages of spermatogenesis.

The fate of SSCs is tightly regulated by many paracrine and autocrine factors. GDNF, which is produced by Sertoli cells in the testis, is the first identified essential growth factor for the *in vivo* and *in vitro* self-renewal of SSCs. RA, the active metabolites of retinol, has long been known as the critical factor for meiosis initiation. Recently, we have shown that RA is sufficient for inducing cultured mouse SSCs to turn into leptotene/zygotene spermatocytes, and it regulates not only meiotic genes but also genes involved in spermatogonial proliferation and differentiation, and even genes involved in the postmeiotic development of spermatogenic cells (4). In the present study, we have identified in SSCs a fate decision regulatory network, which consists of signaling molecules such as GDNF and RA, miR-202 and a large number of target genes including cell cycle regulators and RNA binding proteins. Future studies shall be directed to add in missing links, to identify key nodes and to develop interfering means for this network in order to establish a more efficient *in vitro* spermatogenesis model through a better understanding of the regulatory network.

SUPPLEMENTARY DATA

Supplementary Data are available at NAR Online.

ACKNOWLEDGEMENTS

The authors thank Dr. Yangming Wang in Beijing Key Laboratory of Cardiometabolic Molecular Medicine, Institute of Molecular Medicine, Peking University for critical reading of the manuscript. The authors also thank Jifeng Wang in the Laboratory of Proteomics of Core facilities for Protein Science, Institute of Biophysics, CAS, for technical support.

FUNDING

Ministry of Science and Technology of China [2013CB945001, 2015CB943002, 2016YFC1000600, 2012CB966803 and 2014CBA02003]; National Natural Science Foundation of China [31271379, 31471349,

31670185]; Novo Nordisk-CAS Research Fund [NNCAS-2015-11]. Funding for open access charge: Ministry of Science and Technology of China [2016YFC1000600, 2015CB943002, 2013CB945001, 2012CB966803 and 2014CBA02003].
Conflict of interest statement. None declared.

REFERENCES

1. Griswold,M.D. (2016) Spermatogenesis: the commitment to meiosis. *Physiol. Rev.*, **96**, 1–17.
2. de Rooij,D.G. and Griswold,M.D. (2012) Questions about spermatogonia posed and answered since 2000. *J. Androl.*, **33**, 1085–1095.
3. Manku,G. and Culty,M. (2015) Mammalian gonocyte and spermatogonia differentiation: recent advances and remaining challenges. *Reproduction*, **149**, R139–R157.
4. Wang,S., Wang,X., Ma,L., Lin,X., Zhang,D., Li,Z., Wu,Y., Zheng,C., Feng,X., Liao,S. *et al.* (2016) Retinoic acid is sufficient for the in vitro induction of mouse spermatocytes. *Stem Cell Rep.*, **7**, 80–94.
5. Busada,J.T. and Geyer,C.B. (2016) The role of retinoic acid (RA) in spermatogonial differentiation. *Biol. Reprod.*, **94**, 10.
6. Chalmel,F. and Rolland,A.D. (2015) Linking transcriptomics and proteomics in spermatogenesis. *Reproduction*, **150**, R149–R157.
7. Hayashi,K., Lopes,S.M.C.D., Kaneda,M., Tang,F.C., Hajkova,P., Lao,K.Q., O'Carroll,D., Das,P.P., Tarakhovsky,A., Miska,E.A. *et al.* (2008) MicroRNA biogenesis is required for mouse primordial germ cell development and spermatogenesis. *Plos One*, **3**, e1738.
8. Maatouk,D.M., Loveland,K.L., McManus,M.T., Moore,K. and Harfe,B.D. (2008) Dicer1 is required for differentiation of the mouse male germline. *Biol. Reprod.*, **79**, 696–703.
9. Korhonen,H.M., Meikar,O., Yadav,R.P., Papaioannou,M.D., Romero,Y., Da Ros,M., Herrera,P.L., Toppari,J., Nef,S. and Kotaja,N. (2011) Dicer is required for haploid male germ cell differentiation in mice. *Plos One*, **6**, e24821.
10. Romero,Y., Meikar,O., Papaioannou,M.D., Conne,B., Grey,C., Weier,M., Pralong,F., De Massy,B., Kaessmann,H., Vassalli,J.D. *et al.* (2011) Dicer1 depletion in male germ cells leads to infertility due to cumulative meiotic and spermiogenic defects. *Plos One*, **6**, e25241.
11. Chang,Y.F., Lee-Chang,J.S., Imam,J.S., Buddavarapu,K.C., Subaran,S.S., Sinha-Hikim,A.P., Gorospe,M. and Rao,M.K. (2012) Interaction between microRNAs and actin-associated protein Arpc5 regulates translational suppression during male germ cell differentiation. *Proc. Natl. Acad. Sci. U.S.A.*, **109**, 5750–5755.
12. Wu,Q.X., Song,R., Ortogero,N., Zheng,H.L., Evanoff,R., Small,C.L., Griswold,M.D., Namekawa,S.H., Royo,H., Turner,J.M. *et al.* (2012) The RNase III enzyme DROSHA is essential for microRNA production and spermatogenesis. *J. Biol. Chem.*, **287**, 25173–25190.
13. Zimmermann,C., Romero,Y., Warnefors,M., Bilican,A., Borel,C., Smith,L.B., Kotaja,N., Kaessmann,H. and Nef,S. (2014) Germ cell-specific targeting of DICER or DGCR8 reveals a novel role for endo-siRNAs in the progression of mammalian spermatogenesis and male fertility. *Plos One*, **9**, e107023.
14. McIver,S.C., Roman,S.D., Nixon,B. and McLaughlin,E.A. (2012) miRNA and mammalian male germ cells. *Hum. Reprod. Update*, **18**, 44–59.
15. Holt,J.E., Stanger,S.J., Nixon,B. and McLaughlin,E.A. (2016) Non-coding RNA in spermatogenesis and epididymal maturation. *Adv. Exp. Med. Biol.*, **886**, 95–120.
16. Smorag,L., Zheng,Y., Nolte,J., Zechner,U., Engel,W. and Pantakani,D.V.K. (2012) MicroRNA signature in various cell types of mouse spermatogenesis: evidence for stage-specifically expressed miRNA-221, -203 and -34b-5p mediated spermatogenesis regulation. *Biol. Cell*, **104**, 677–692.
17. Tong,M.H., Mitchell,D., Evanoff,R. and Griswold,M.D. (2011) Expression of Mirlet7 Family microRNAs in response to retinoic acid-induced spermatogonial differentiation in mice. *Biol. Reprod.*, **85**, 189–197.
18. Yang,Q.E., Racicot,K.E., Kaucher,A.V., Oatley,M.J. and Oatley,J.M. (2013) MicroRNAs 221 and 222 regulate the undifferentiated state in mammalian male germ cells. *Development*, **140**, 280–290.
19. He,Z.P., Jiang,J.J., Kokkinaki,M., Tang,L., Zeng,W.X., Gallicano,I., Dobrinski,I. and Dym,M. (2013) MiRNA-20 and mirna-106a regulate spermatogonial stem cell renewal at the post-transcriptional level via targeting STAT3 and Ccnd1. *Stem Cells*, **31**, 2205–2217.
20. Huszar,J.M. and Payne,C.J. (2013) MicroRNA 146 (Mir146) modulates spermatogonial differentiation by retinoic acid in mice. *Biol. Reprod.*, **88**, 15.
21. Yu,Z.R., Raabe,T. and Hecht,N.B. (2005) MicroRNA Mirn122a reduces expression of the posttranscriptionally regulated germ cell transition protein 2 (Tnp2) messenger RNA (mRNA) by mRNA cleavage. *Biol. Reprod.*, **73**, 427–433.
22. Dai,L.S., Tsai-Morris,C.H., Sato,H., Villar,J., Kang,J.H., Zhang,J.B. and Dufau,M.L. (2011) Testis-specific miRNA-469 up-regulated in gonadotropin-regulated testicular RNA helicase (GRTH/DDX25)-null mice silences transition protein 2 and protamine 2 messages at sites within coding region: implications of its role in germ cell development. *J. Biol. Chem.*, **286**, 44306–44318.
23. Bjork,J.K., Sandqvist,A., Elsing,A.N., Kotaja,N. and Sistonen,L. (2010) miR-18, a member of Oncomir-1, targets heat shock transcription factor 2 in spermatogenesis. *Development*, **137**, 3177–3184.
24. Tong,M.H., Mitchell,D.A., McGowan,S.D., Evanoff,R. and Griswold,M.D. (2012) Two miRNA clusters, Mir-17-92 (Mirc1) and Mir-106b-25 (Mirc3) are involved in the regulation of spermatogonial differentiation in mice. *Biol. Reprod.*, **86**, 72.
25. Bao,J.Q., Li,D., Wang,L., Wu,J.W., Hu,Y.Q., Wang,Z.G., Chen,Y., Cao,X.K., Jiang,C.Z., Yan,W. *et al.* (2012) MicroRNA-449 and microRNA-34b/c function redundantly in murine testes by targeting E2F transcription factor-retinoblastoma protein (E2F-pRb) pathway. *J. Biol. Chem.*, **287**, 21686–21698.
26. Ro,S., Park,C., Sanders,K.M., McCarrey,J.R. and Yan,W. (2007) Cloning and expression profiling of testis-expressed microRNAs. *Dev. Biol.*, **311**, 592–602.
27. Yan,N.H., Lu,Y.L., Sun,H.Q., Tao,D.C., Zhang,S.Z., Liu,W.Y. and Ma,Y.X. (2007) A microarray for microRNA profiling in mouse testis tissues. *Reproduction*, **134**, 73–79.
28. Yan,N.H., Lu,Y.L., Sun,H.Q., Qiu,W.M., Tao,D.C., Liu,Y.Q., Chen,H.J., Yang,Y., Zhang,S.Z., Li,X. *et al.* (2009) Microarray profiling of microRNAs expressed in testis tissues of developing primates. *J. Assist. Reprod. Genet.*, **26**, 179–186.
29. Luo,L.F., Ye,L.Z., Liu,G., Shao,G.C., Zheng,R., Ren,Z.Q., Zuo,B., Xu,D.Q., Lei,M.G., Jiang,S.W. *et al.* (2010) Microarray-based approach identifies differentially expressed microRNAs in porcine sexually immature and mature testes. *Plos One*, **5**, e11744.
30. Marcon,E., Babak,T., Chua,G., Hughes,T. and Moens,P.B. (2008) miRNA and piRNA localization in the male mammalian meiotic nucleus. *Chromosome Res.*, **16**, 243–260.
31. Stanton,J.-A.L., Buchold,G.M., Coarfa,C., Kim,J., Milosavljevic,A., Gunaratne,P.H. and Matzuk,M.M. (2010) Analysis of microRNA expression in the prepubertal testis. *PLos One*, **5**, e15317.
32. Niu,Z.Y., Goodyear,S.M., Rao,S., Wu,X., Tobias,J.W., Avarbock,M.R. and Brinster,R.L. (2011) MicroRNA-21 regulates the self-renewal of mouse spermatogonial stem cells. *Proc. Natl. Acad. Sci. U.S.A.*, **108**, 12740–12745.
33. Gan,H.Y., Lin,X.W., Zhang,Z.Q., Zhang,W., Liao,S.Y., Wang,L.X. and Han,C.S. (2011) piRNA profiling during specific stages of mouse spermatogenesis. *RNA*, **17**, 1191–1203.
34. Kuchen,S., Resch,W., Yamane,A., Kuo,N., Li,Z.Y., Chakraborty,T., Wei,L., Laurence,A., Yasuda,T., Peng,S.Y. *et al.* (2010) Regulation of microRNA expression and abundance during lymphopoiesis. *Immunity*, **32**, 828–839.
35. Kanatsu-Shinohara,M., Ogonuki,N., Inoue,K., Miki,H., Ogura,A., Toyokuni,S. and Shinohara,T. (2003) Long-term proliferation in culture and germline transmission of mouse male germline stem cells. *Biol. Reprod.*, **69**, 612–616.
36. Kubota,H., Avarbock,M.R. and Brinster,R.L. (2004) Culture conditions and single growth factors affect fate determination of mouse spermatogonial stem cells. *Biol. Reprod.*, **71**, 722–731.
37. Wang,S., Wang,X., Wu,Y. and Han,C. (2015) IGF-1R signaling is essential for the proliferation of cultured mouse spermatogonial stem cells by promoting the G2/M progression of the cell cycle. *Stem Cells Dev.*, **24**, 471–483.
38. Hukema,R.K., Buijsen,R.A.M., Raske,C., Severijnen,L.A., Nieuwenhuizen-Bakker,I., Minneboo,M., Maas,A., de Crom,R.,

Kros,J.M., Hagerman,P.J. *et al.* (2014) Induced expression of expanded CGG RNA causes mitochondrial dysfunction in vivo. *Cell Cycle*, **13**, 2600–2608.
39. Wang,T., Wei,J.J., Sabatini,D.M. and Lander,E.S. (2014) Genetic screens in human cells using the CRISPR-Cas9 system. *Science*, **343**, 80–84.
40. Gropp,M. and Reubinoff,B. (2006) Lentiviral vector-mediated gene delivery into human embryonic stem cells. *Methods Enzymol.*, **420**, 64–81.
41. Wisniewski,J.R., Zougman,A., Nagaraj,N. and Mann,M. (2009) Universal sample preparation method for proteome analysis. *Nat. Methods*, **6**, U359–U360.
42. Huang,D.W., Sherman,B.T. and Lempicki,R.A. (2008) Systematic and integrative analysis of large gene lists using DAVID bioinformatics resources. *Nat. Protoc.*, **4**, 44–57.
43. Sambrook,J. and Russell,D.W.(2006) Isolation of DNA from mammalian cells grown in 96-well microtiter plates. *Cold Spring Harb. Protoc.*, doi:10.1101/pdb.prot3695.
44. Fu,H.J., Zhu,L., Yang,M., Zhang,Z.Y., Tie,Y., Jiang,H., Sun,Z.X. and Zheng,X.F. (2006) A novel method to monitor the expression of microRNAs. *Mol. Biotechnol.*, **32**, 197–204.
45. Cabili,M.N., Trapnell,C., Goff,L., Koziol,M., Tazon-Vega,B., Regev,A. and Rinn,J.L. (2011) Integrative annotation of human large intergenic noncoding RNAs reveals global properties and specific subclasses. *Genes Dev.*, **25**, 1915–1927.
46. Zhong,X.M., Li,N., Liang,S., Huang,Q.H., Coukos,G. and Zhang,L. (2010) Identification of microRNAs regulating reprogramming factor LIN28 in embryonic stem cells and cancer cells. *J. Biol. Chem.*, **285**, 41961–41971.
47. Zhang,Y., Zheng,D.Y., Xiong,Y., Xue,C.B., Chen,G., Yan,B.B. and Ye,Q.F. (2014) miR-202 suppresses cell proliferation in human hepatocellular carcinoma by downregulating LRP6 post-transcriptionally. *FEBS Lett.*, **588**, 1913–1920.
48. Sun,Z.W., Zhang,T.Q., Hong,H.Y., Liu,Q.X. and Zhang,H.G. (2014) miR-202 suppresses proliferation and induces apoptosis of osteosarcoma cells by downregulating Gli2. *Mol. Cell. Biochem.*, **397**, 277–283.
49. Bisio,A., De Sanctis,V., Del Vescovo,V., Denti,M.A., Jegga,A.G., Inga,A. and Ciribilli,Y. (2013) Identification of new p53 target microRNAs by bioinformatics and functional analysis. *BMC Cancer*, **13**, 552.
50. Cheung,T.H. and Rando,T.A. (2013) Molecular regulation of stem cell quiescence. *Nat. Rev. Mol. Cell Biol.*, **14**, 329–340.
51. Sada,A., Suzuki,A., Suzuki,H. and Saga,Y. (2009) The RNA-binding protein NANOS2 is required to maintain murine spermatogonial stem cells. *Science*, **325**, 1394–1398.
52. Costoya,J.A., Hobbs,R.M., Barna,M., Cattoretti,G., Manova,K., Sukhwani,M., Orwig,K.E., Wolgemuth,D.J. and Pandolfi,P.P. (2004) Essential role of Plzf in maintenance of spermatogonial stem cells. *Nat. Genet.*, **36**, 653–659.
53. Bruscoli,S., Velardi,E., Di Sante,M., Bereshchenko,O., Venanzi,A., Coppo,M., Berno,V., Mameli,M.G., Colella,R., Cavaliere,A. *et al.* (2012) Long glucocorticoid-induced leucine zipper (L-GILZ) protein interacts with Ras protein pathway and contributes to spermatogenesis control. *J. Biol. Chem.*, **287**, 1242–1251.
54. Liao,H.F., Chen,W.S.C., Chen,Y.H., Kao,T.H., Tseng,Y.T., Lee,C.Y., Chiu,Y.C., Lee,P.L., Lin,Q.J., Ching,Y.H. *et al.* (2014) DNMT3L promotes quiescence in postnatal spermatogonial progenitor cells. *Development*, **141**, 2402–2413.
55. Zhang,Y., Wang,S., Wang,X.X., Liao,S.Y., Wu,Y.J. and Han,C.S. (2012) Endogenously produced FGF2 is essential for the survival and proliferation of cultured mouse spermatogonial stem cells. *Cell Res.*, **22**, 773–776.
56. Kubota,H., Avarbock,M.R. and Brinster,R.L. (2004) Growth factors essential for self-renewal and expansion of mouse spermatogonial stem cells. *Proc. Natl. Acad. Sci. U.S.A.*, **101**, 16489–16494.
57. Tay,J. and Richter,J.D. (2001) Germ cell differentiation and synaptonemal complex formation are disrupted in CPEB knockout mice. *Dev. Cell*, **1**, 201–213.